·特邀综述·

# 基于激光晶体的固态波导激光器

陈峰*, 李子琦

山东大学物理学院,晶体材料国家重点实验室, 山东 济南 250100

**摘要** 光波导是集成光学中的基本元件之一,构建于光波导结构上的波导激光器是一种微型激光源,近年来受到较多研究人员的关注,并有望在未来光子学系统中发挥重要的作用。激光晶体是固态激光器的主要增益介质之一。本文综述了基于激光晶体的固态波导激光器的最新研究进展,包括连续波波导激光器和脉冲波导激光器(调 $Q$ 或锁模),其工作波长涵盖了从可见光到中红外的各个波段;还对波导激光研究的未来发展方向进行了展望。

**关键词** 激光器; 光波导; 波导激光; 激光晶体; 连续波激光; 调 $Q$ 激光; 锁模激光

**中图分类号** O436 **文献标志码** A **doi**: 10.3788/CJL202047.0500008

# Solid-State Waveguide Lasers Based on Laser Crystals

Chen Feng*, Li Ziqi

*State Key Laboratory of Crystal Materials, School of Physics, Shandong University, Jinan, Shandong* 250100, *China*

**Abstract** Optical waveguides are fundamental elements in integrated optics. Compact lasers based on the waveguide platforms are miniature light sources that have gained increasing research attention. Waveguide lasers are expected to play important roles in photonics. Laser crystals are major gain media for solid-state lasers. In this study, we review the state-of-the-art advances in solid-state waveguide lasers, including operation of continuous wave and pulse ($Q$-switched or mode-locked). The lasing wavelength covers a wide spectral range from visible light to the mid-infrared. Furthermore, a brief perspective on future research directions is provided.

**Key words** lasers; optical waveguide; waveguide laser; laser crystal; continuous-wave laser; $Q$-switched laser; mode-locked laser

**OCIS codes** 140.3460; 230.7370; 140.3540; 140.4050

## 1 引 言

光波导是折射率较高的区域被折射率较低的区域包围所形成的一种微纳光子学结构,可以实现对光的无衍射长距离传输,是集成光子学系统中的基本元件之一。按照结构对光传输进行限制的维度来划分,光波导包括具有一维限制的平面(平板)光波导和具有二维限制的通道光波导。固态光波导横截面的尺寸在微米乃至亚微米量级,因此固态光波导可用于提高微纳光学器件的集成度,在集成光子学领域有着广阔的应用前景。激光波导的基本基质材料包括单晶硅等半导体,以及玻璃、介电晶体、陶瓷等绝缘体,此外还有一些有机材料(如聚合物等)。介电晶体种类繁多,功能各异,在光波导器件的制备与应用中发挥了非常重要的作用。目前,人们已经利用多种技术在介电晶体材料中制备了光波导结构,如飞秒激光直写、离子注入、离子交换等。按照功能分类,常见的晶体种类包括激光晶体、非线性晶体、电光晶体、声光晶体等。基于不同功能光学材料的光波导可用于制备多种功能性的光学器件,如耦合器、分束器、放大器、激光器、调制器与频率转换器等[1-6]。最近,光波导在量子信息技术领域也扮演着非常重要的角色,例如,在三维波导芯片中,实现了量子随机行走[7]和光子轨道角动量的高保真传输[8]。基于波导区域相对较高的光密度,其光学效应(如非线性响应)与体块材料相比,通常有着明显的提升。这些显著的特点使得基于光波导的光子学元件在集成光路中发挥着基础和关键的作用。

**收稿日期**: 2020-01-06; **修回日期**: 2020-02-20; **录用日期**: 2020-03-09

**基金项目**: 国家自然科学基金(11535008,11274203)

* **E-mail**: drfchen@sdu.edu.cn

固态波导激光器是基于激光材料光波导的微型激光源，具有体积小、稳定性高、易于集成等优势，固态波导激光器的研发为光子学系统中可集成、高效率的激光光源提供了一种可能的选择方案。与体块材料相比，由于光被限制在微米量级的空间范围内传输，波导中较高的光密度降低了激光振荡的阈值，提高了激光输出的斜效率。相较于光纤激光器，固态波导激光器有着更加紧凑的结构，同时相较于半导体激光器具有较小的光束发散角。此外，波导激光可以在不同的波导结构中实现，如直线型、弯曲型和分束型等结构。利用具有特殊结构的光波导可以实现对激光光束的三维空间调控。根据工作方式的不同，波导激光器可分为连续波波导激光器和脉冲波导激光器。结合不同特点的晶体材料及非线性光学材料（如二维材料、碳纳米管和纳米颗粒等），研究人员已经成功地在波导基质平台中实现了调 $Q$ 和锁模脉冲激光的输出，推动了超快激光源在紧凑型激光源方向的发展。在生物医学领域，固态激光波导与微流控通道的集成可以实现对肿瘤细胞与葡萄糖溶液的精准探测[9]，进一步拓展了波导激光的应用范围。

Grivas[10-11]和陈峰课题组[12]分别对平面波导激光和脉冲波导激光的研究进展进行了较为系统的总结。近几年来，随着波导制备技术的成熟，以及纳米技术的蓬勃发展，国内外在波导激光领域的多个方向取得了一系列重要进展。本课题组在固态激光光波导的制备、连续波波导激光器，以及脉冲波导激光器等方向开展了大量研究工作。本文结合近年来本课题组的研究工作，对国内外波导激光领域的新进展进行了介绍和综述，主要包括激光晶体波导的制备，基于新晶体和新结构的波导激光，以及在不同工作模式和工作波长下的波导激光，并对其未来发展前景进行了展望。

## 2　基于激光晶体的光波导

激光工作物质是激光器的三要素之一。通常而言，全固态波导激光器的增益介质需要具备如下几个特点：1）荧光发射谱线强度较强；2）在泵浦波段有较高的吸收系数；3）对应跃迁有较高的荧光量子效率。激光晶体中掺杂的主要激活离子通常为 $Nd^{3+}$、$Er^{3+}$、$Yb^{3+}$、$Pr^{3+}$、$Tm^{3+}$ 与 $Ho^{3+}$ 等，它们在不同的介质材料中表现出不同的物理和光学特性。钇铝石榴石（YAG）系列材料是常见的激光工作物质之一，其中掺钕钇铝石榴石（Nd∶YAG）是应用最为广泛的激光增益介质，此外还有掺铒钇铝石榴石（Er∶YAG）、掺镱钇铝石榴石（Yb∶YAG）和掺铥钇铝石榴石（Tm∶YAG）等。掺杂钒酸盐晶体系列也是常用的激光工作物质，主要包括钒酸钇晶体（$YVO_4$）、钒酸钆晶体（$GdVO_4$）和钒酸镥晶体（$LuVO_4$）等。其中掺钕钒酸钇晶体（Nd∶$YVO_4$）由于具有较宽、较大的吸收截面和发射截面而成为应用最为广泛的激光晶体之一，目前绝大多数绿光激光笔就是采用 Nd∶$YVO_4$ 作为激光增益介质。此外，常见的晶体还包括过渡金属（Cr、Ti、Co）掺杂的激光晶体，如红宝石（Cr∶$Al_2O_3$）、绿宝石（Cr∶$BeAl_2O_4$）和掺钛蓝宝石（Ti∶$Al_2O_3$）等，其中 Ti∶$Al_2O_3$ 是可调波长固态激光器（700～1000 nm）的主要增益介质。

飞秒激光直写技术可以使材料内部或表面具有较为复杂的三维微纳结构，是制备激光晶体光波导的有效方法之一[2,13-17]。近年来，运用飞秒激光直写方法，研究人员已经在包括 Nd∶YAG 在内的20多种激光晶体中制备了不同结构的光波导结构。如图 1 所示，陈峰课题组[12,18]利用飞秒激光直写技术在 Nd∶YAG 晶体中制备出了类光子晶格结构的包层光波导，并对其导波特性进行了详细的研究。飞秒激光脉冲通过物镜会聚在晶体内部，通过电脑程序控制 $XYZ$ 三维电动平台移动来实现三维结构的写入。由于焦点处具有较高的能量密度，飞秒脉冲通过非线性吸收过程（包括过多光子吸收、隧穿电离和雪崩电离等）沉积到材料内部，引发局域性的晶格结构（折射率）变化。通过不同参数的飞秒激光（脉宽、重复频率、写入速度、深度、脉冲能量、激光波长、偏振等）和不同材料的相互作用，可以制备多种类型的光波导结构。根据折射率变化和波导结构的不同，光波导主要分为以下三种类型：基于 I 类改性（折射率升高）的 I 类光波导，通过飞秒激光聚焦诱导区域的折射率升高，即写入区域即为波导区域；基于 II 类改性（折射率降低）的双线型光波导，通过飞秒激光脉冲写入两条折射率降低的痕迹（Track），痕迹之间的区域的折射率因飞秒激光诱导应力场的改变而升高，该区域成为波导核心；由一系列 II 类改性区域环绕所形成的相对折射率较高的导波结构称为 III 类光波导，又称为包层光波导。

载能离子束辐照技术也是一种常用的晶体光波导制备方法[1,19-20]。该技术的制备原理如下：注入离子与材料晶格相互作用，离子能量发生沉积，引发局域化的晶格畸变，从而诱导晶体折射率发生相应的改变。应用载能离子束辐照技术可以制备出均

匀、大面积的平面光波导结构。此外，结合掩模板、精密金刚石刀切割、超快激光刻蚀等技术还可以进一步形成条形或脊形的光波导结构。图 2 所示为结合离子注入和精密金刚石刀切割在 Nd∶YAG 晶体中同时制备脊形波导和 Ag 纳米颗粒的示意图。除此之外，还有一些其他的制备方法也可以实现光波导的制备，如离子交换、脉冲激光沉积、分子束外延、液相外延等，但每种方法的适用范围不一样，其适用范围与晶体材料本身的物理属性及化学属性有很大关系。

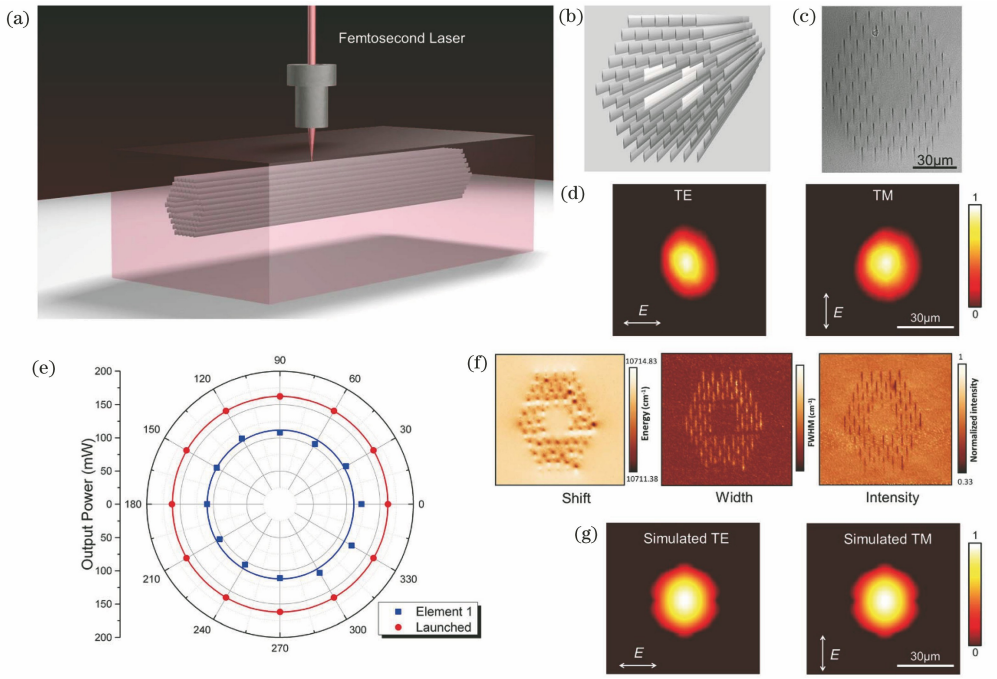


图 1　飞秒激光直写 Nd∶YAG 晶体光波导的制备与表征[18]。(a)飞秒激光直写光波导示意图；(b)所制备光子微结构示意图；(c)端面显微照片；(d)导波模式；(e)波导的偏振依赖特性；(f)共聚焦荧光映像；(g)仿真的导波模式

Fig. 1　Preparation and characterization of femtosecond laser writing Nd∶YAG optical waveguide[18]. (a) Schematic of femtosecond laser direct writing optical waveguide; (b) schematic of prepared photonic microstructure; (c) microscope image of cross section; (d) guided mode; (e) polarization dependence of waveguide; (f) confocal fluorescence mapping; (g) simulated waveguide mode

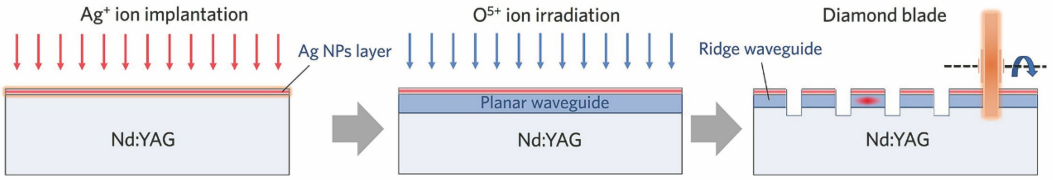


图 2　在 Nd∶YAG 晶体中制备脊形波导和 Ag 纳米粒子的示意图[21]

Fig. 2　Schematic of fabrication of ridge waveguide and Ag nanoparticles in Nd∶YAG crystal[21]

## 3　基于光波导的紧凑型激光器

固态波导激光器可以与某些多功能光子器件兼容，为集成光子学开辟了新的发展机遇。基于光波导平台的激光器主要分为两类：连续波波导激光器和脉冲波导激光器。根据工作模式的不同，脉冲波导激光器又可以进一步分为调 $Q$ 波导激光器和锁模波导激光器。在这一节中，主要按照激光的工作方式介绍波导激光的近期研究进展。

### 3.1　连续波模式工作的波导激光器

连续波波导激光器具有稳定的工作状态，国内外许多课题组已经基于不同结构的光波导实现了多种工作波长的连续激光的输出[22-43]。研究人员利用固态激光波导实现了高功率、高斜效率的激光输出。Grant-Jacob 等[44]基于 Yb∶YAG 平面波导实现了平均功率达11.5 W 的连续激光输出。Tan 等[45]实现了斜效率高达 70% 的 Nd∶$GdVO_4$ 波导激光的输出。基于 Nd∶YAP 类光子晶格结构的包层波导，

Nie 等[46]实现了 1072/1079 nm 双波长激光的输出，并且输出的两波长功率对比与泵浦光的偏振态密切相关。激光晶体与新型导波结构的结合可以实现对激光光束的三维空间调控。如图 3 所示，陈峰课题组[47]用飞秒激光直写技术在 Nd∶YAG 晶体中制备了具有不同分束比(0°、0.5°、1°、2°)的 Y 分支型包层波导，同时支持 TM 和 TE 偏振，并实现了波长为 1.06 μm 的连续波激光振荡，基于分束比为 0.5° 的波导激光的最大输出功率为 0.2 W，最大斜效率为 20%。Jia 等[48]制备了一种可以调控光场的类光子晶格波导结构，在 808 nm 激光泵浦下，基于 1×2 与 1×4 波导分支器实现了连续波波导激光的输出。

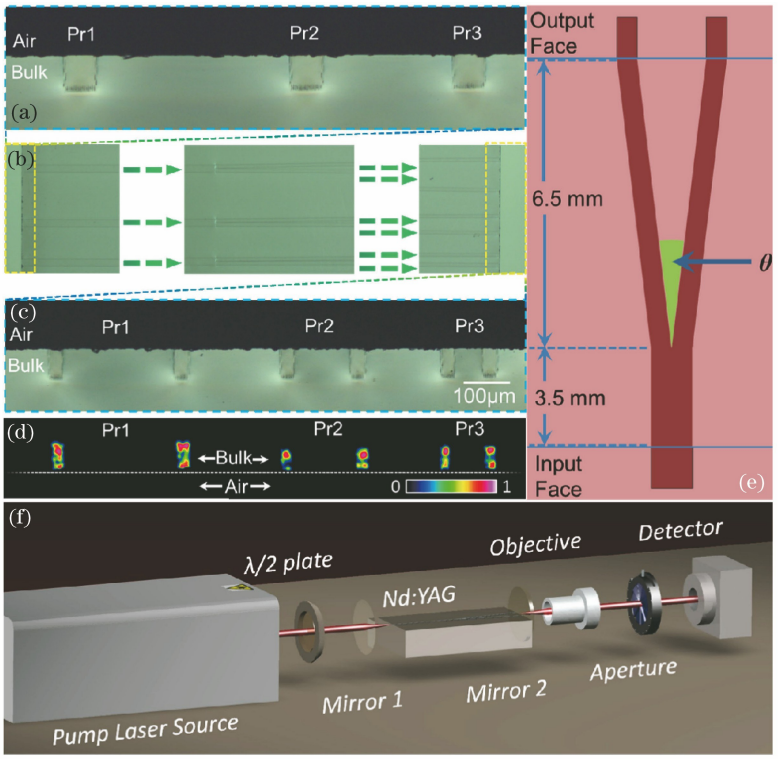


图 3　基于 Nd∶YAG 晶体的 Y 分支连续波波导激光器[47]。(a)入射端面的显微镜照片；(b)上表面的显微镜照片；(c)出射端面的显微镜照片；(d)激光模式图；(e)波导结构示意图；(f)波导激光实验装置图

Fig. 3　Y-branch continuous wave guided lasers based on Nd∶YAG[47]. (a) Microscope image of input face; (b) microscope image of upper surface; (c) microscope image of output face; (d) laser patterns; (e) schematic of waveguide structure; (f) experimental setup of waveguide laser

Calmano 课题组[49]利用飞秒激光直写技术在 Yb∶YAG 晶体中制备了弯曲型通道光波导结构，并实现了连续波波导激光的输出。如图 4 所示，该工作与使用标准程序写入的波导不同的是，采用了一种新的波导制备方案，即采用线性平移与垂直于平移方向的曲折运动叠加的方法写入，可以增大写入痕迹(弯曲部分处)的相对折射率差。利用基于这种方法制作的直波导，实现了斜效率高达 79%的连续

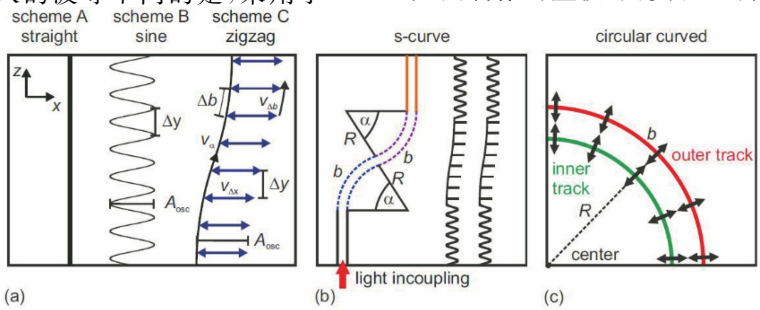


图 4　波导制备方案[49]。(a)三种波导制备方案；(b) S 弯曲形波导；(c)圆弧状波导

Fig. 4　Waveguide fabrication schemes[49]. (a) Three waveguide fabrication schemes; (b) S-bend waveguide; (c) circular waveguide

波波导激光输出，平均功率大于 1 W，是目前文献中所报道的最高斜效率波导激光。对于曲率半径 $R \geqslant 20$ mm 的弯曲波导激光器，斜效率高达 50%～60%，进一步证实了飞秒激光写入法制备复杂光学器件的可能性。

工作在可见光波段的激光器在高速通讯、数据存储与生物医疗等领域有着广阔的应用前景。基于光波导平台，人们同样实现了可见光波段连续激光的输出[50]。在可见光波段，激光增益介质主要是掺杂镨离子（$Pr^{3+}$）的激光晶体，如 Pr∶$LiYF_4$、Pr∶$LiLuF_4$、Pr∶$KYF_4$、Pr∶$YAlO_3$ 与 Pr∶$SrAl_{12}O_{19}$ 等。Calmano 等[51]应用飞秒激光直写技术在 Pr∶$SrAl_{12}O_{19}$ 晶体中制备出了 II 类双线型光波导，并输出了平均功率 28.1 mW、波长 643.5 nm 的红色激光。Reichert 等[52]在 Pr、Mg∶$SrAl_{12}O_{19}$ 晶体光波导中实现了绿光（525.3 nm）、红光（644.0 nm）和深红光（724.9 nm）波段的连续波导激光输出，且最大功率分别达到了 36，1065，504 mW。可见波段激光也可以在平面波导中实现[53]。通过 479.2 nm 半导体激光器泵浦，Bolaños 等[54]基于液相外延法制备的 Pr∶$LiYF_4$ 通道型光波导结构同时实现了绿色、橙色和红色的光波导激光输出。如图 5 所示，在 639 nm 和 604 nm 波长处的激光最大斜效率分别为 40.4% 和 32%[54]。

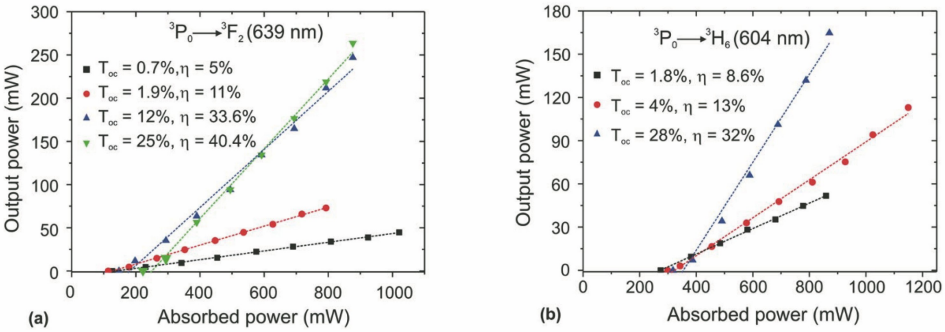


图 5　基于 Pr∶$LiYF_4$ 晶体的波导激光实验结果[54]。(a) 639 nm；(b) 604 nm

Fig. 5　Experimental results of waveguide laser based on Pr∶$LiYF_4$ crystal[54]. (a) 639 nm; (b) 604 nm

工作在中红外波段的激光器在空间通讯、大气环境监测、激光雷达、激光医疗等多个领域有着广阔的应用前景。在此波段，增益介质通常为掺激活离子 $Ho^{3+}$ 和 $Tm^{3+}$ 等的晶体。Lancaster 等[55]在 Ho、Tm∶ZBLAN 玻璃中利用飞秒激光直写技术成功制备出了包层光波导，随后，通过 790 nm 的激光泵浦，实现了波长为 2052 nm 的连续波波导激光输出，斜效率和输出功率分别达到了 20% 和 76 mW。Lancaster 等[56]利用基于 Ho∶ZBLAN 玻璃制备的包层波导实现了2.9 μm 的连续波激光输出。通过进一步调整激光谐振腔[57]，2.1 μm 波长下的连续波波导激光最大平均输出功率可以达到 1.1 W，斜效率为 51%。Kar 课题组[58]进一步报道了平均输出功率为 2 W 的 Ho∶YAG 波导激光器。基于 Tm∶$LiYF_4$ 平面光波导，Bolanos 等[28]报道了 1.9 μm 连续波波导激光器。Kar 课题组[59]基于 Cr∶ZnS 包层光波导实现了2333 nm 波长的激光输出。近期，Mateos 课题组[60]报道了利用飞秒激光直写技术在 Ho∶$KGd(WO_4)_2$ 中制备的包层光波导，传输损耗低至 0.94 dB/cm，如图 6 所示，通过半导体二极管

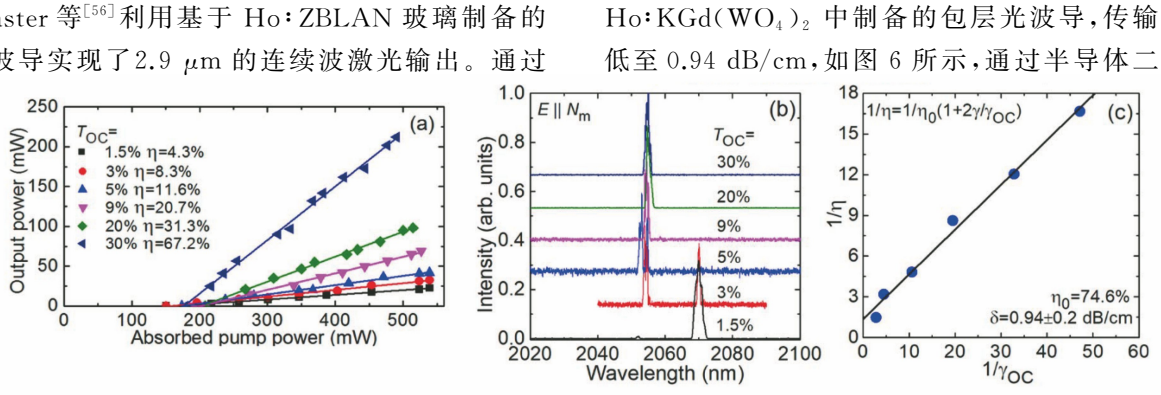


图 6　带内泵浦 Ho∶$KGd(WO_4)_2$ 波导激光器[60]。(a)泵浦功率与输出功率的关系图；(b)波导输出激光光谱；(c)波导损耗

Fig. 6　In-band pumped Ho∶$KGd(WO_4)_2$ waveguide lasers[60]. (a) Output power versus absorbed pump power; (b) waveguide output laser spectra; (c) loss of waveguide

泵浦实现了斜效率为67.2%、工作波长为2.1 μm的连续波波导激光输出。

本文对近期波导连续激光的实验结果进行了汇总，详见表1。

表1　近期关于连续波波导激光器的实验结果

Table 1　Recent experimental results for continuous-wave waveguide lasers

| Gain media | Method | Waveguide configuration | Wavelength / nm | Lasing threshold / mW | Slope efficiency / % | Max output power / mW | Ref. |
|---|---|---|---|---|---|---|---|
| Nd:YAG | Fs laser writing | Cladding | 1064 | 95.6 | 44 | 181 | [61] |
| Nd:YAG | Fs laser writing | Cladding | 1064 | 101 | 46.1 | 384 | [62] |
| Nd:YAG | Ion irradiation/ fs laser ablation | Ridge | 1064 | 39 | 35 | 20 | [63] |
| Nd:YAG | Ion irradiation/ fs laser ablation | Ridge | 1064 | 64.9 | 42.5 | 46 | [64] |
| Nd:YAG | Ion irradiation/ diamond blade dicing | Ridge | 1064 | 79 | 43 | 84 | [65] |
| Nd:$YVO_4$ | Ion irradiation | Planar | 1067 | 9.3 | 8.5 | 3 | [66] |
| Nd:$YVO_4$ | Fs laser writing | Cladding | 1064 | 138 | 65 | 335 | [67] |
| Nd:GGG | Fs laser writing | Dual line | 1061 | 29 | 25 | 11 | [26] |
| Nd:$GdVO_4$ | Fs laser writing | Dual line | 1063.6 | 52 | 70 | 256 | [45] |
| Nd:$GdVO_4$ | Fs laser writing | Cladding | 1064.5 | 92 | 52.3 | 430 | [68] |
| Nd:$GdVO_4$ | Fs laser writing | Cladding | 1064 | 178 | 68 | 570 | [69] |
| Nd:$LuVO_4$ | Fs laser writing | Dual line | 1066.4 | 98 | 14 | 30 | [70] |
| Nd:KGW | Fs laser writing | Dual line | 1065 | 141 | 52.3 | 33 | [71] |
| Nd:GGG | Fs laser writing | Cladding | 1063 | 270 | 44.4 | 209 | [72] |
| Nd:GGG | Ion irradiation/ fs laser ablation | Ridge | 1063 | 71.6 | 41.8 | 25 | [73] |
| Nd:LGS | Fs laser writing | Cladding | 1068 | 54 | 24 | 16 | [74] |
| Nd:YAP | Fs laser writing | Cladding | 1072/1079 | 384.5 | 30.9 | 101.3 | [46] |
| Yb:YAG | Pulsed laser deposition | Planar | 1030 | 3200 | 48 | 11500 | [44] |
| Yb:YAG | Fs laser writing | Dual line | 1030 | 181 | 51 | 1760 | [75] |
| Yb:YAG | Fs laser writing | Dual line | 1030 | 245 | 75 | 1200 | [76] |
| Yb:YAG | Fs laser writing | Cladding | 1030 | 392 | 62.9 | 80.2 | [77] |
| Yb:YAG | Fs laser writing | Cladding | 1030 | 141 | 79 | 1000 | [49] |
| Yb:$KY(WO_4)_2$ | Ion irradiation | Stripe | 1025 | 5.5 | 76 | 650 | [78] |
| Cr:ZnS | Fs laser writing | Cladding | 2333 | 450 | 20 | 101 | [59] |
| Ho:$KGd(WO_4)_2$ | Fs laser writing | Cladding | 2055 | 180 | 67.2 | 212 | [60] |
| Ho:YAG | Fs laser writing | Cladding | 2096 | 100 | 16 | 1775 | [58] |
| Ho:ZBLAN | Fs laser writing | Cladding | 2070 | 110 | 51 | 1100 | [57] |
| Ho:ZBLAN | Fs laser writing | Cladding | 2900 | 27.2 | 16.7 | 25 | [56] |
| Tm:$KY(WO_4)_2$ | Liquid phase epitaxy | Stripe | 1842 | 25 | 70 | 300 | [79] |
| Tm:$KY(WO_4)_2$ | Liquid phase epitaxy | Stripe | 1840 | 50 | 80 | 1600 | [80] |
| Tm:$Y_2O_3$ | Pulsed laser deposition | Planar | 1950 | 50 | 9 | 35 | [81] |
| Tm:YAG | Fs laser writing | Cladding | 1985 | 312 | 27 | 660 | [82] |
| Tm:ZBLAN | Fs laser writing | Cladding | 1880 | 21 | 50 | 47 | [25] |
| Ho,Tm:ZBLAN | Fs laser writing | Cladding | 2052 | 20 | 20 | 100 | [55] |
| Ti:sapphire | Fs laser writing | Dual line | 798.25 | 84 | 23.5 | 143 | [30] |
| Pr:$YLiF_4$ | Liquid phase epitaxy | Planar | 639 | 324 | 5 | 25 | [53] |
| Pr:$YLiF_4$ | Liquid phase epitaxy | Planar | 604 | 527 | 6 | 12 | [53] |
| Pr:$YLiF_4$ | Liquid phase epitaxy | Stripe | 604 | 250 | 32 | 165 | [54] |
| Pr:$YLiF_4$ | Liquid phase epitaxy | Stripe | 639 | 200 | 40.4 | 165 | [54] |
| Pr:$SrAl_{12}O_{19}$ | Fs laser writing | Dual line | 643.5 | 190 | 8 | 28.1 | [51] |

### 3.2　脉冲模式工作的波导激光器

为了获得更高的峰值功率和更窄的脉宽，近年来越来越多的工作聚焦于波导脉冲激光器的研究[12]。根据激光器工作模式的不同，可以进一步将波导脉冲激光器分为调 $Q$ 波导激光器和锁模波导激光器。其中饱和吸收体在波导脉冲激光的产生过程中起到了重要的作用。常见的饱和吸收体主要有半导体可饱和吸收镜（SESAM）和低维纳米材料。SESAM 具有高的损伤阈值和空气稳定性，是目前商业上最常用的可饱和吸收体。但 SESAM 有其固有的缺点，如工作波长范围窄、制备成本高等。近年来，新型低维纳米材料特别是二维材料因具有宽工作波段、低成本、易制备、恢复时间快、饱和强度低等特点[83-93]，被广泛应用于脉冲激光器中。二维材料主要包括石墨烯、过渡金属二硫化物和黑磷等[94]，其非线性饱和吸收的主要机制是泡利不相容原理。对于金属纳米粒子，其主要机制是入射光电场与导带表面电子相互作用产生局域表面等离激元共振效应。低维纳米材料与光波导的结合，推动超快激光源朝着紧凑型和可集成化的方向发展。

被动调 $Q$ 是在波导中产生高脉冲能量的纳秒级激光脉冲的有效方法。利用饱和吸收体的非线性光学作用，可以将激光谐振腔的品质因数 $Q$ 从一个较低的值调制到很高的数值，从而储存在腔内的能量会以短脉冲的形式被迅速释放，输出一个高能量脉冲。基于光波导的调 $Q$ 激光器主要使用掺 $Nd^{3+}$、$Yb^{3+}$ 或 $Er^{3+}$ 的增益介质来产生近红外激光，及掺杂 $Ho^{3+}$ 或 $Tm^{3+}$ 的增益介质来产生中红外激光。Bae 等[95]基于 Yb∶KluW 晶体波导与单壁碳纳米管饱和吸收体实现了1040 nm 的调 $Q$ 激光输出。Ma 等[96]报导了基于 Yb∶YSGG 脊形波导的1024 nm被动调 $Q$ 激光器。Cheng 等[97]基于 Nd∶YAG 包层波导得到了新型饱和吸收体二硒化锡（$SnSe_2$）调制的 1 μm 调 $Q$ 波导激光器，随着泵浦功率的增加，其重复频率从 0.337 MHz 提升至 2.294 MHz。如图 7 所示，Hakobyan 等[98]实现了高功率 Yb∶YAG 通道波导调 $Q$ 激光器，平均输出功率超过 5.6 W，斜效率达到 74%。该工作通过垂直外腔面发射半导体激光器泵浦与 SESAM 调制来实现调 $Q$ 激光的运转，最大重复频率为 5.4 MHz，脉冲宽度为 11 ns，最大脉冲能量达到了 1 μJ。近期，陈峰课题组[99]实现了基于 Nd∶$YVO_4$ 包层波导和 graphene/$WS_2$ 二维异质结材料的 1 μm 调 $Q$ 脉冲输出。相比单一二维材料，由于 graphene/$WS_2$ 的层间电荷转移过程具有更高的非线性响应，将 graphene/$WS_2$ 异质结应用于飞秒激光加工的 Nd∶$YVO_4$ 晶体包层波导平台中作为可饱和吸收体，实现了比将单一 graphene 或 $WS_2$ 材料作为饱和吸收体时更高斜效率（37%）与单脉冲能量（33.1 nJ）的波导调 $Q$ 脉冲激光输出。同时，陈峰课题组[100]通过将固态激光波导与外部电控制元件相结合，实现了不同工作模式的切换和不同脉宽激光的输出，进一步提升了波导激光器的集成度和可调控性。此外，Fuerbach 课题组[101]首次将变形螺旋铁电液晶与激光波导相结合，实现了超紧凑型主动调 $Q$ 波导激光器，重复频率可调谐范围为 0.1～20 kHz。

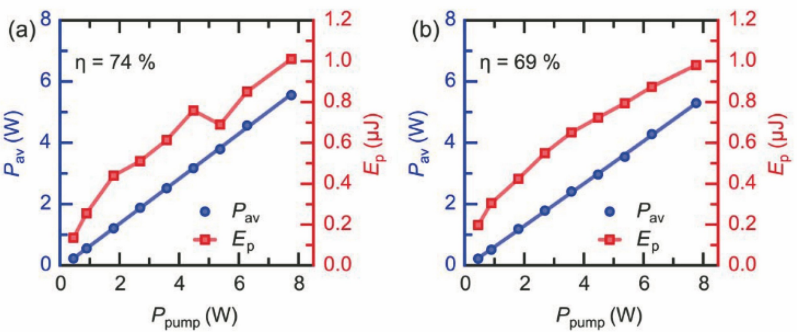


图 7　基于 Yb∶YAG 波导的调 $Q$ 激光器的平均输出功率和脉冲能量随泵浦功率的变化[98]。(a)无空气间隙；(b)有空气间隙

Fig. 7　Average output power and pulse energy of the $Q$-switched lasers based on Yb∶YAG waveguide as a function of pump power [98]. (a) Without airgap aligning; (b) with airgap aligning

低维材料与光波导的结合方式主要有两种：透射模式和倏逝场耦合模式。不同的耦合模式可以实现不同强度的光场，如图 8 所示，Kim 等[102]对 Yb∶KYW 平面波导与碳纳米管的两种不同结合方式的调 $Q$ 性能进行了比较。在相同的腔结构下，对碳纳米管沉积在输入镜（M 层）、输出耦合器（OC 层）和平面波导顶面（WG 层）三种情况下的激光性能进行了详细的分析。根据实验结果及计算的腔内束流尺寸和电

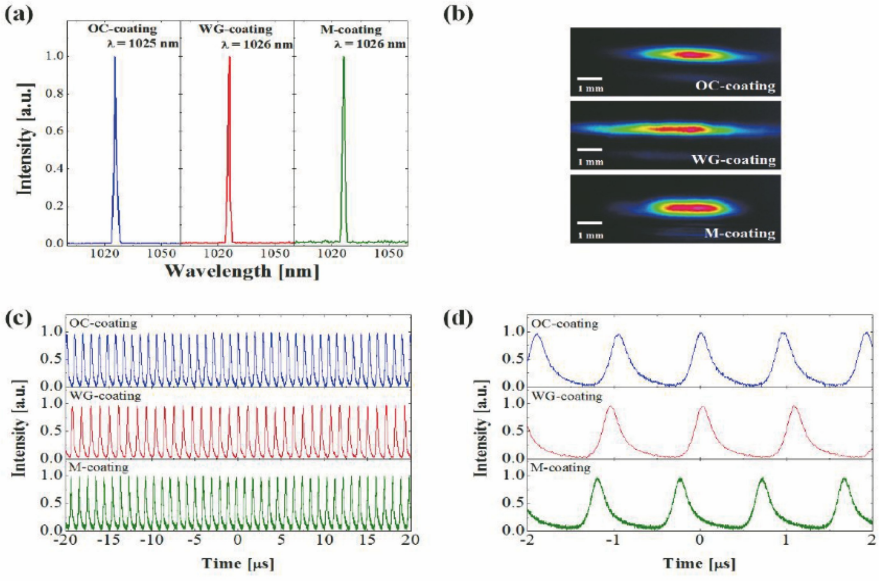


图 8　基于 Yb∶KYW 平面波导的调 $Q$ 激光性能[102]。(a)发射光谱;(b)激光模式图;(c)在 40 μs 时间尺度的脉冲序列;(d)在 4 μs 时间尺度的脉冲序列

Fig. 8　Performances of $Q$-switched laser based on Yb∶KYW planar waveguide[102]. (a) Emission spectra; (b) laser modes; (c) pulse trains in 40 μs time span; (d) pulse trains in 4 μs time span

场分布,基于倏逝场耦合的方案相对透射模式可以在较低的饱和强度下实现稳定的调 $Q$ 脉冲输出。

基于中红外波导平台的调 $Q$ 波导激光器也取得一系列研究进展。Mateos 课题组[103]利用飞秒激光直写技术在 Tm∶KLu$(WO_4)_2$ 晶体中制备了表面包层光波导,结合碳纳米管饱和吸收体实现了中红外波段的调 $Q$ 激光输出,1847.4 nm 处的最大输出功率达到 171.1 mW,脉冲持续时间可短至50 ns,重复频率高达 1.48 MHz,如图 9 所示。基于石墨烯和二硫化钼饱和吸收体,Kifle 等[104]进一步在 1849.6 nm波长下实现了斜效率 48.7%、最短脉宽 66 ns 的调 $Q$ 波导脉冲激光。基于 $Sb_2Te_3$ 薄膜的倏逝场相互作用,Loiko 等[105]也实现了 2 μm 被动调 $Q$ 波导激光器,单脉冲能量可以达到 3.5 μJ。

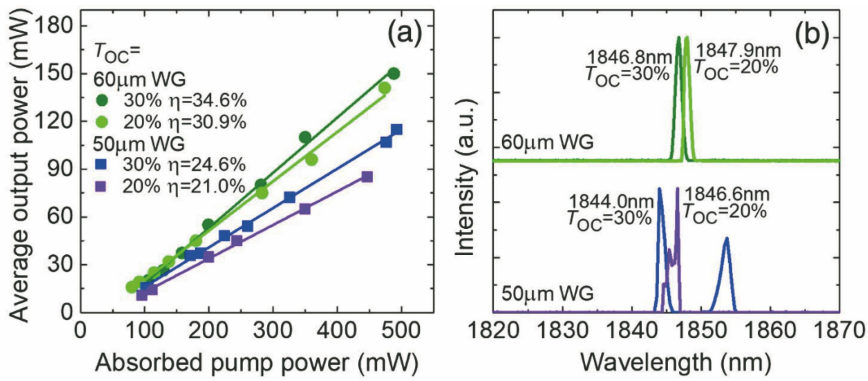


图 9　基于 Tm∶KLuW 表面包层波导的调 $Q$ 激光器性能[103]。(a)平均输出功率与泵功功率的关系图;(b)激光发射光谱

Fig. 9　$Q$-switched lasers performance based on Tm∶KLuW surface cladding waveguide[103]. (a) Output power versus absorbed pump power; (b) laser emission spectra

表 2 汇总了国内外近期关于波导调 Q 激光器的实验结果。

应用被动锁模技术可以在波导平台中实现脉冲宽度在皮秒或飞秒量级的脉冲激光输出。通常所采用的饱和吸收体为快饱和吸收体,即它们具有非常短的上能级寿命。近年来,具有高重复频率(尤其是重复频率在 1 GHz 以上)的波导锁模激光器受到越来越多的关注,在很多领域有着巨大的应用价值,比如高速光通信系统、光学频率梳及高速光学采样等。锁模波导激光器的重复频率 $f_{rep}$ 的计算式为

表 2　调 $Q$ 光波导激光器实验结果汇总

Table 2　Summary of experimental results for $Q$-switched waveguide lasers

| Gain media | Method | Waveguide configuration | Saturable absorber | Wavelength / nm | Pulse width / ns | Frequency / MHz | Pulse energy / nJ | Ref. |
|---|---|---|---|---|---|---|---|---|
| Nd∶YAG | Ion irradiation | Planar | Graphene | 1064 | 9800 | 0.0029 | 370 | [106] |
| Nd∶YAG | Vacuum sintering | Planar | Graphene oxide | 1064 | 179 | 0.93 | 221 | [107] |
| Nd∶YAG | Ion irradiation | Stripe | Graphene | 1064 | 57 | 4.1 | 77 | [108] |
| Nd∶YAG | Ion irradiation | Stripe | $WS_2$ | 1064 | 70 | 6.10 | | [109] |
| Nd∶YAG | Ion irradiation | Stripe | black phosphorous | 1064 | 55 | 5.6 | | [109] |
| Nd∶YAG | Fs laser writing | Cladding | Graphene | 1064 | 55 | 10.3 | 4.6 | [110] |
| Nd∶YAG | Fs laser writing | Cladding | Graphene | 1064 | 70 | 4.3 | 55 | [18] |
| Nd∶YAG | Fs laser writing | Cladding | Graphene | 1064 | 90 | 3.0 | 63 | [111] |
| Nd∶YAG | Fs laser writing | Cladding | $MoS_2$ | 1064 | 203 | 1.10 | 112 | [112] |
| Nd∶YAG | Fs laser writing | Cladding | Graphene | 1064 | 40 | | | [100] |
| Nd∶YAG | Fs laser writing | Cladding | Graphene/$WSe_2$ | 1064 | 43.4 | | | [113] |
| Nd∶YAG | Fs laser writing | Cladding | $MoSe_2$ | 1064 | 80 | 3.334 | 36 | [114] |
| Nd∶YAG | Fs laser writing | Cladding | $WSe_2$ | 1064 | 52 | 2.938 | 19 | [114] |
| Nd∶YAG | Fs laser writing | Cladding | $SnSe_2$ | 1064 | 129 | 2.294 | 44.5 | [97] |
| Nd∶YAG | Ion irradiation | Stripe | $Bi_2Se_3$ | 1064 | 46 | 4.7 | 31.3 | [115] |
| Nd∶YAG | Fs laser writing | Cladding | $Bi_2Se_3$ | 1064 | 45 | | | [116] |
| Nd∶YAG | Ion irradiation/ diamond blade dicing | Ridge | $WS_2$ | 1064 | 125 | 0.36 | | [96] |
| Nd∶YAG | Ion irradiation/ fs laser writing | Ridge | Graphene | 1064 | 99 | 2.9 | 14 | [117] |
| Nd∶$YVO_4$ | Ion irradiation | Stripe | $WS_2$ | 1064 | 52 | | | [118] |
| Nd∶$YVO_4$ | Fs laser writing | Dual line | Graphene | 1064 | 25 | 16.3 | 8.1 | [119] |
| Nd∶$YVO_4$ | Fs laser writing | Cladding | $WS_2$ | 1064 | 51 | 2.3 | | [120] |
| Nd∶$YVO_4$ | Fs laser writing | Cladding | Graphene/$WS_2$ | 1064 | 66 | 7.777 | 33.1 | [99] |
| Nd∶$YVO_4$ | Fs laser writing | Cladding | Ag∶$LiNbO_3$ | 1064 | | | 38 | [121] |
| Nd∶$YVO_4$ | Fs laser writing | Cladding | Graphene | 1064 | 30 | 5.3 | | [120] |
| Nd∶$YVO_4$ | Fs laser writing | Cladding | Graphene | 1064 | 31.2 | 14.5 | 26.8 | [122] |
| Nd∶$GdVO_4$ | Fs laser writing | Cladding | Graphene | 1064 | 75 | 18 | 19 | [69] |
| Yb∶YAG | Fs laser writing | Dual line | SESAM | 1030 | 11 | 5.4 | 1000 | [98] |
| Yb∶YAG | Fs laser writing | Dual line | Carbon nanotubes | 1029 | 78 | 1.59 | 37.7 | [123] |
| Yb∶$Y_2O_3$ | Pulsed laser deposition | Planar | Graphene | 1064 | 121 | 1.47 | 330 | [124] |
| Yb,Na∶$CaF_2$ | Fs laser writing | Cladding | Graphene | 1013.9/1027.9 | 103.4 | 0.2693 | 130 | [125] |
| Tm∶KYW | Liquid phase epitaxy | Planar | Graphene | 1831.8 | 195 | 1.13 | 5.8 | [126] |
| Tm∶KYW | Fs laser writing | Cladding | Graphene | 1917 | 136 | 0.37 | 1200 | [127] |
| Tm∶KLuW | Fs laser writing | Cladding | Graphene | 1846.1 | 72 | 1.45 | 13.1 | [104] |
| Tm∶KYW | Fs laser writing | Cladding | Carbon nanotubes | 1912 | 50 | 1.48 | 7 | [128] |
| Tm∶KYW | Fs laser writing | Cladding | Carbon nanotubes | 1846.8 | 98 | 1.42 | 105.6 | [103] |
| Tm∶KYW | Liquid phase epitaxy | Planar | Carbon nanotubes | 1837.1 | 83 | 1.39 | 33 | [129] |
| Yb∶KYW | Liquid phase epitaxy | Planar | Carbon nanotubes | 1026 | 215 | 1.103 | 22 | [102] |
| Yb∶KLuW | Fs laser writing | Cladding | Carbon nanotubes | 1040 | 88.5 | 1.16 | 613 | [95] |
| Tm∶KLuW | Fs laser writing | Cladding | $MoS_2$ | 1845 | 66 | 1.51 | 12 | [130] |

$$f_{\mathrm{rep}}=\frac{c}{2nl},\tag{1}$$

式中：$c$ 为光速，$n$ 为波导的有效折射率，$l$ 为腔长。因为基于波导平台的谐振腔通常较短，所以波导锁模激光器的重复频率通常在千兆赫兹(GHz)量级。

目前，锁模波导激光器的研究主要集中在调 $Q$ 锁模(QML)上，其中主要应用的可饱和吸收体为石墨烯材料。Kar 课题组[131]报道了基于 Yb∶BG 玻璃包层、重复频率 1.5 GHz 的 QML 波导激光器，得到了中心波长 1039 nm、脉宽 1.06 ps 的激光脉冲。Ren

等[132]基于 Tm:YAG 包层波导展示了波长为2 μm 的被动调 $Q$ 锁模激光器，重复频率为 7.8 GHz，平均输出功率为 6.5 mW。Thorburn 等[133]应用 Ho:YAG 包层波导在～2.1 μm 波段实现了 5.9 GHz 的调 $Q$ 锁模激光运转。近期，陈峰课题组[134]将石墨烯、二硫化钼和铋烯三种典型二维材料作为超快可饱和吸收体，运用端面耦合技术，在飞秒激光加工制备的 Nd:$YVO_4$ 晶体微纳光波导中实现了 6.5 GHz 超高基频重复频率的锁模脉冲激光输出，信噪比均大于 50 dB，最短脉冲宽度达到了 26 ps。此外，利用银纳米颗粒的场增强效应可以显著提升石墨烯的非线性光学性能[135]，修饰后石墨烯的饱和强度降低为原来的 1/57，调制深度增大了 19 倍。如图 10 所示，基于这些优异的非线性性质，将修饰后的石墨烯作为可饱和吸收体可以得到更短的锁模脉冲，即 33 ps，小于石墨烯调制的 52 ps。

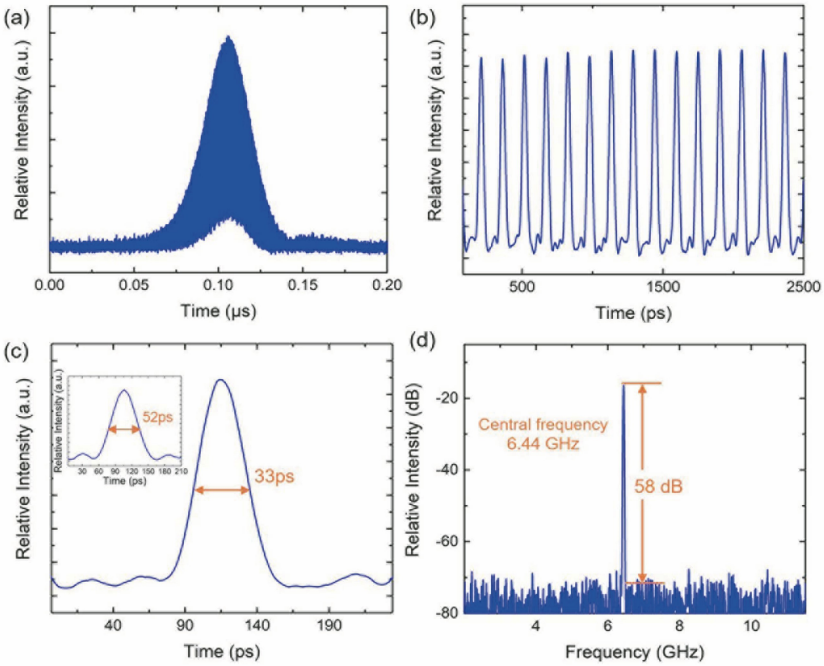


图 10　基于 Nd:$YVO_4$ 包层波导的调 $Q$ 锁模激光器的性能曲线[135]。
(a)调 $Q$ 包络；(b)锁模脉冲序列；(c)单个锁模脉冲；(d)射频频谱图

Fig. 10　Performances of $Q$-switched mode-locked lasers based on Nd:$YVO_4$ cladding waveguide[135].
(a) $Q$-switched envelope; (b) mode-locked pulse trains; (c) single mode-locked pulse; (d) radio frequency spectrum

贵金属纳米粒子因具有局域表面等离激元共振效应，可以显著增强周围基质的非线性光学性质，有利于微纳光子器件的单片集成。应用离子束技术可以合成嵌入型金属纳米颗粒或纳米棒，通过调控介质种类，及注入金属纳米颗粒的种类、大小、形状、深度、浓度等来调控其光学性质。陈峰课题组[136]系统地研究了金离子注入法制备的铌酸锂($LiNbO_3$)晶体中金纳米粒子的超快非线性光学响应。$Z$ 扫描结果表明，嵌入金纳米粒子的 $LiNbO_3$ 晶体在近红外 1 μm 波段具有超快可饱和吸收特性。如图 11 所示，将嵌有金纳米粒子的 $LiNbO_3$ 晶片作为可饱和吸收体应用于激光写入的 Nd:$YVO_4$ 波导平台中，实现了 1064 nm 的稳定调 $Q$ 锁模脉冲输出，重复频率为 6.4 GHz，脉宽为 74.1 ps。同时，利用倏逝场相互作用，可以进一步实现固态激光波导和纳米颗粒饱和吸收体的单片集成[21]。近期，陈峰课题组[137]通过操控嵌入的 Ag 纳米颗粒阵列的间距，增强了熔融石英玻璃在近红外波段的非线性光学响应，实现了 1 μm 的调 $Q$ 锁模脉冲输出。

基于光波导平台，有几项工作实现了基于可饱和吸收体的连续锁模(CWML)激光。Okhrimchuk 等[138]报道了基于 Nd:YAG 包层波导的连续锁模激光，脉冲宽度为 16 ps，重复频率高达 11 GHz。陈峰课题组[139]报道了基于 $ReSe_2$ 新型饱和吸收体的连续锁模波导激光器，产生了脉冲宽度 29 ps、工作频率 6.5 GHz 的超高重复频率的脉冲激光。如图 12 所示，Choi 等[140]报道了基于 Yb:YAG 双线型光波导与碳纳米管的2.08 GHz 连续锁模激光器，平均输出功率为 322 mW，最短脉冲宽度为 2 ps，该工作通过引入 Gires-Tournois 干涉镜对波导色散进行了补偿。Khurmi 等[141]基于 Er:glass、Yb:glass 包层波导实现了最短脉宽达180 fs 的连续锁模激光，线

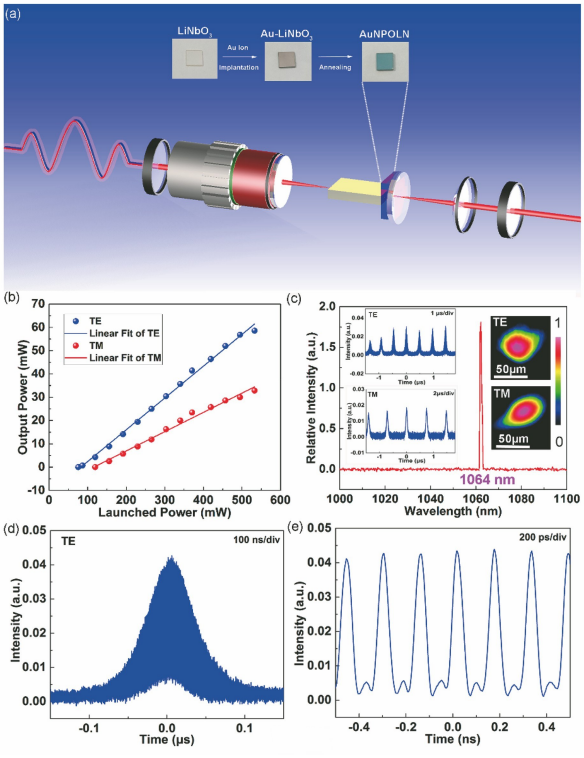


图 11　基于嵌入金纳米颗粒的铌酸锂饱和吸收体的调 $Q$ 锁模波导激光器[136]。

(a)实验装置;(b)输出功率与泵浦功率的关系图;(c)测量的激光发射光谱;(d)调 $Q$ 脉冲包络;(e)锁模脉冲序列

Fig. 11　$Q$-switched mode-locked waveguide lasers based on $LiNbO_3$ saturable absorber embedded with gold nanoparticles[136]. (a) Schematic of experimental setup; (b) output power versus pump power; (c) measured emission spectrum; (d) $Q$-switched pulse envelope; (e) mode-locked pulse train

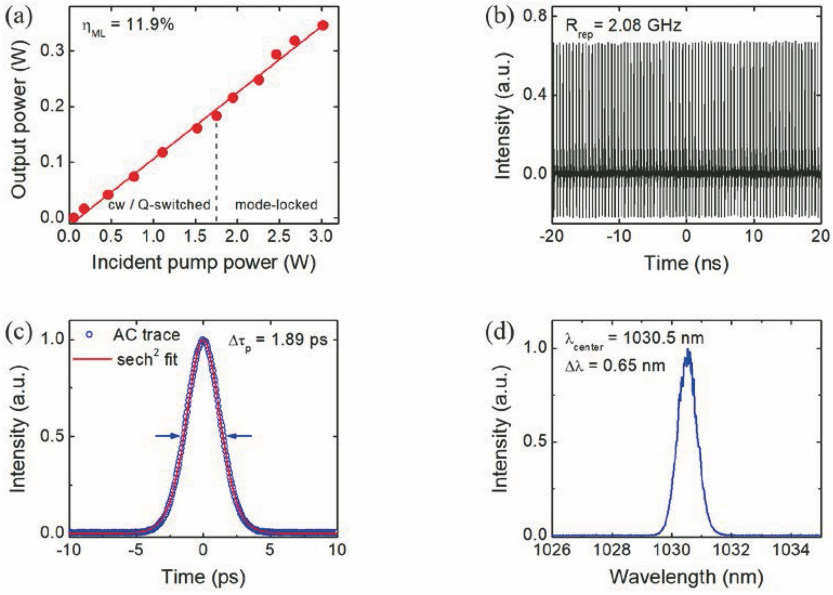


图 12　基于 Yb∶YAG 双线型波导的连续波锁模激光特性[140]。

(a)输出功率与泵浦功率的关系图;(b)锁模脉冲序列;(c)自相关曲线图;(d)激光发射光谱

Fig. 12　Characteristics of the continuous-wave mode-locked laser based on Yb∶YAG dual-line waveguide[140]. (a) Output power versus pump power; (b) mode-locked pulse train; (c) autocorrelation trace; (d) laser emission spectroscopy

宽为25 nm,重复频率为 156 MHz。近期,Grivas 课题组[142]基于石墨烯饱和吸收体和飞秒激光写入的 Ti∶sapphire 双线型波导实现了脉宽41.4 fs、重复频率 21.25 GHz 的连续锁模脉冲输出,为目前基于波

导激光所实现的最短脉冲，通过使用光纤梳状滤波器，激光工作频率可进一步倍增至 42.5 GHz。

表 3 汇总了国内外关于波导锁模激光器的参数对比。

表 3　基于光波导的锁模激光器实验结果汇总

Table 3　Summary of experimental results for mode-locked waveguide lasers

| Gain media | Method | Waveguide configuration | Saturable absorber | Operation regime | Wavelength / nm | Pulse width / ps | Frequency / GHz | Ref. |
|---|---|---|---|---|---|---|---|---|
| Nd∶YAG | Fs laser writing | Cladding | Cu∶LN | QML | 1064 | 55 | 8.6 | [143] |
| Nd∶YAG | Fs laser writing | Cladding | Ag∶YAG | QML | 1064 | 29.5 | 10.53 | [21] |
| Nd∶YAG | Fs laser writing | Cladding | Cu∶LT | QML | 1064 | 23.5 | 8.6 | [144] |
| Nd∶YAG | Fs laser writing | Cladding | $PtSe_2$ | QML | 1064 | 27 | 8.8 | [145] |
| Nd∶YAG | Fs laser writing | Cladding | Graphene | CWML | 1064 | 16.7 | 11 | [138] |
| Nd∶YAG | Fs laser writing | Cladding | Graphene | CWML | 1061/1064 | 20 | 9.8 | [146] |
| Nd∶$YVO_4$ | Fs laser writing | Cladding | Modified graphene | QML | 1064 | 33 | 6.5 | [135] |
| Nd∶$YVO_4$ | Fs laser writing | Cladding | $ReSe_2$ | CWML | 1064 | 29 | 6.5 | [139] |
| Nd∶$YVO_4$ | Fs laser writing | Cladding | $MoS_2$ | QML | 1064 | 43 | 6.5 | [134] |
| Nd∶$YVO_4$ | Fs laser writing | Cladding | $Bi_2Se_3$ | QML | 1064 | 26 | 6.5 | [134] |
| Nd∶$YVO_4$ | Fs laser writing | Cladding | Au∶LN | QML | 1064 | 74.1 | 6.5 | [136] |
| Nd∶$YVO_4$ | Fs laser writing | Cladding | Ag∶$SiO_2$ | QML | 1064 | 27.4 | 6.5 | [137] |
| Nd∶$YVO_4$ | Fs laser writing | Cladding | $WSe_2$ | QML | 1064 | 47 | 6.5 | [147] |
| Tm∶YAG | Fs laser writing | Cladding | Graphene | QML | 1943.5 | ～70 | 7.8 | [132] |
| Ho∶YAG | Fs laser writing | Cladding | Graphene | QML | 2091 | ～100 | 5.9 | [133] |
| Yb∶YAG | Fs laser writing | Dual line | Carbon nanotubes | CWML | 1030.3 | 1.89 | 2.08 | [140] |
| Yb∶glass | Fs laser writing | Dual line | Graphene | QML | 1039 | 1.06 | 1.5 | [131] |
| Yb∶glass | Ion exchange | Strip | SESAM | CWML | 1058 | 0.8 | 4.9 | [148] |
| Yb∶glass | Ion exchange | Strip | SESAM | CWML | 1041.4 | 0.811 | 15.2 | [149] |
| Er,Yb∶glass | Ion exchange | Strip | Graphene | QML | 1535 | ～70 | 6.8 | [150] |
| Er,Yb∶glass | Fs laser writing | Cladding | SESAM | CWML | 1550 | 0.18 | 0.156 | [141] |
| Tm∶ZBLAN | Fs laser writing | Cladding | $Bi_2Te_3$ | QML | ～1875 | ～700 | 0.436 | [151] |

## 4　总结与展望

本文综述了基于光波导平台激光器的最新研究进展。通过飞秒激光直写、离子注入和离子交换等方法可以制备不同结构的光波导，基于不同激光晶体的光波导可以实现不同波段的激光输出。结合饱和吸收体的非线性调制，可以进一步实现调 $Q$ 或锁模波导激光运转。波导激光器有望在未来集成光子学系统中发挥重要的作用。为了进一步推动波导激光器的发展，还有几个方面有待进一步探索。例如，为了实现基于波导平台的连续锁模激光器，可以选用激光发射截面大的激光晶体作为增益介质，制备较小尺寸的波导来降低激光模式尺寸，通过优化波导制备工艺来降低波导的损耗，寻找性能更优的低维材料可饱和吸收体，以及在激光谐振腔内加入色散补偿元件等。此外，基于波导平台实现可见光波段的脉冲激光输出具有重要意义，也是未来激光领域的一个研究热点。

## 参　考　文　献


[1] Chen F. Micro- and submicrometric waveguiding structures in optical crystals produced by ion beams for photonic applications[J]. Laser & Photonics Reviews, 2012, 6(5): 622-640.

[2] Chen F, Vázquez de Aldana J R. Optical waveguides in crystalline dielectric materials produced by femtosecond-laser micromachining[J]. Laser & Photonics Reviews, 2014, 8(2): 251-275.

[3] Tang H, di Franco C, Shi Z Y, et al. Experimental quantum fast hitting on hexagonal graphs[J]. Nature Photonics, 2018, 12(12): 754-758.

[4] Li L Q, Nie W J, Li Z Q, et al. Laser-writing of ring-shaped waveguides in BGO crystal for telecommunication band[J]. Optics Express, 2017, 25(20): 24236-24241.

[5] Li Z Q, Cheng C, Romero C, et al. Low-loss optical waveguides in $\beta$-BBO crystal fabricated by femtosecond-laser writing[J]. Optical Materials,

2017, 73: 45-49.

[6] Nie W J, Jia Y C, Vázquez de Aldana J R, et al. Efficient second harmonic generation in 3D nonlinear optical-lattice-like cladding waveguide splitters by femtosecond laser inscription[J]. Scientific Reports, 2016, 6: 22310.

[7] Tang H, Lin X F, Feng Z, et al. Experimental two-dimensional quantum walk on a photonic chip [J]. Science Advances, 2018, 4(5): eaat3174.

[8] Chen Y, Gao J, Jiao Z Q, et al. Mapping twisted light into and out of a photonic chip[J]. Physical Review Letters, 2018, 121(23): 233602.

[9] Li G H, Li H Y, Gong R M, et al. Intracavity biosensor based on the Nd∶YAG waveguide laser: tumor cells and dextrose solutions[J]. Photonics Research, 2017, 5(6): 728-732.

[10] Grivas C. Optically pumped planar waveguide lasers, part I: fundamentals and fabrication techniques[J]. Progress in Quantum Electronics, 2011, 35(6): 159-239.

[11] Grivas C. Optically pumped planar waveguide lasers: part II: gain media, laser systems, and applications[J]. Progress in Quantum Electronics, 2016, 45/46: 3-160.

[12] Jia Y C, Chen F. Compact solid-state waveguide lasers operating in the pulsed regime: a review [Invited][J]. Chinese Optics Letters, 2019, 17(1): 012302.

[13] Gattass R R, Mazur E. Femtosecond laser micromachining in transparent materials[J]. Nature Photonics, 2008, 2(4): 219-225.

[14] Choudhury D, MacDonald J R, Kar A K. Ultrafast laser inscription: perspectives on future integrated applications[J]. Laser & Photonics Reviews, 2014, 8(6): 827-846.

[15] Sugioka K, Cheng Y. Ultrafast lasers: reliable tools for advanced materials processing [J]. Light: Science & Applications, 2014, 3(4): e149.

[16] Jia Y C, Chen F. Advances in dielectric crystal waveguides produced by direct femtosecond laser writing [J]. Laser & Optoelectronics Progress, 2016, 53(1): 010001.
贾曰辰, 陈峰. 飞秒激光直写介电晶体光波导的研究进展[J]. 激光与光电子学进展, 2016, 53(1): 010001.

[17] Shi Y, Xu B, Wu D, et al. Research progress on fabrication of functional microfluidic chips using femtosecond laser direct writing technology [J]. Chinese Journal of Lasers, 2019, 46(10): 1000001.
史杨, 许兵, 吴东, 等. 飞秒激光直写技术制备功能化微流控芯片研究进展[J]. 中国激光, 2019, 46(10): 1000001.

[18] Jia Y C, Cheng C, Vázquez de Aldana J R, et al. Monolithic crystalline cladding microstructures for efficient light guiding and beam manipulation in passive and active regimes[J]. Scientific Reports, 2015, 4: 5988.

[19] Chen F, Wang X L, Wang K M. Development of ion-implanted optical waveguides in optical materials: a review[J]. Optical Materials, 2007, 29(11): 1523-1542.

[20] Chen F. Photonic guiding structures in lithium niobate crystals produced by energetic ion beams [J]. Journal of Applied Physics, 2009, 106(8): 081101.

[21] Li R, Pang C, Li Z Q, et al. Monolithic waveguide laser mode-locked by embedded Ag nanoparticles operating at 1 μm[J]. Nanophotonics, 2019, 8(5): 859-868.

[22] Geskus D, Aravazhi S, Grivas C, et al. Microstructured $KY(WO_4)_2$∶$Gd^{3+}$, $Lu^{3+}$, $Yb^{3+}$ channel waveguide laser[J]. Optics Express, 2010, 18(9): 8853-8858.

[23] Bradley J D B, Pollnau M. Erbium-doped integrated waveguide amplifiers and lasers [J]. Laser & Photonics Reviews, 2011, 5(3): 368-403.

[24] Calmano T, Paschke A G, Siebenmorgen J, et al. Characterization of an Yb∶YAG ceramic waveguide laser, fabricated by the direct femtosecond-laser writing technique[J]. Applied Physics B, 2011, 103(1): 1-4.

[25] Lancaster D G, Gross S, Ebendorff-Heidepriem H, et al. Fifty percent internal slope efficiency femtosecond direct-written $Tm^{3+}$ ∶ ZBLAN waveguide laser[J]. Optics Letters, 2011, 36(9): 1587-1589.

[26] Zhang C, Dong N N, Yang J, et al. Channel waveguide lasers in Nd∶GGG crystals fabricated by femtosecond laser inscription[J]. Optics Express, 2011, 19(13): 12503-12508.

[27] Ams M, Dekker P, Marshall G D, et al. Ultrafast laser-written dual-wavelength waveguide laser[J]. Optics Letters, 2012, 37(6): 993-995.

[28] Bolanos W, Starecki F, Benayad A, et al. Tm∶$LiYF_4$ planar waveguide laser at 1.9 μm[J]. Optics Letters, 2012, 37(19): 4032-4034.

[29] Cantelar E, Jaque D, Lifante G. Waveguide lasers based on dielectric materials[J]. Optical Materials, 2012, 34(3): 555-571.

[30] Grivas C, Corbari C, Brambilla G, et al. Tunable, continuous-wave Ti∶sapphire channel waveguide lasers written by femtosecond and picosecond laser

pulses[J]. Optics Letters, 2012, 37(22): 4630-4632.

[31] Müller S, Calmano T, Metz P, et al. Femtosecond-laser-written diode-pumped Pr∶$LiYF_4$ waveguide laser [J]. Optics Letters, 2012, 37(24): 5223-5225.

[32] Ter-Gabrielyan N, Fromzel V, Mu X, et al. High efficiency, resonantly diode pumped, double-clad, Er∶YAG-core, waveguide laser [J]. Optics Express, 2012, 20(23): 25554-25561.

[33] Purnawirman, Sun J, Adam T N, et al. C- and L-band erbium-doped waveguide lasers with wafer-scale silicon nitride cavities [J]. Optics Letters, 2013, 38(11): 1760-1762.

[34] Ge L, Li J, Zhou Z W, et al. Fabrication of composite YAG/Nd∶YAG/YAG transparent ceramics for planar waveguide laser [J]. Optical Materials Express, 2014, 4(5): 1042-1049.

[35] Della Valle G, Festa A, Sorbello G, et al. Single-mode and high power waveguide lasers fabricated by ion-exchange[J]. Optics Express, 2008, 16(16): 12334-12341.

[36] Bain F M, Lagatsky A A, Thomson R R, et al. Ultrafast laser inscribed Yb∶$KGd(WO_4)_2$ and Yb∶$KY(WO_4)_2$ channel waveguide lasers [J]. Optics Express, 2009, 17(25): 22417-22422.

[37] Grivas C, Shepherd D P, Eason R W, et al. Room-temperature continuous-wave operation of Ti∶sapphire buried channel-waveguide lasers fabricated via proton implantation[J]. Optics Letters, 2006, 31(23): 3450-3452.

[38] Osellame R, Chiodo N, Della Valle G, et al. Waveguide lasers in the C-band fabricated by laser inscription with a compact femtosecond oscillator [J]. IEEE Journal of Selected Topics in Quantum Electronics, 2006, 12(2): 277-285.

[39] Romanyuk Y E, Borca C N, Pollnau M, et al. Yb-doped $KY(WO_4)_2$ planar waveguide laser [J]. Optics Letters, 2006, 31(1): 53-55.

[40] Della Valle G, Taccheo S, Osellame R, et al. 1.5 μm single longitudinal mode waveguide laser fabricated by femtosecond laser writing[J]. Optics Express, 2007, 15(6): 3190-3194.

[41] Rivier S, Mateos X, Petrov V, et al. Tm∶$KY(WO_4)_2$ waveguide laser[J]. Optics Express, 2007, 15(9): 5885-5892.

[42] Flores-Romero E, Vázquez G V, Márquez H, et al. Planar waveguide lasers by proton implantation in Nd∶YAG crystals[J]. Optics Express, 2004, 12(10): 2264-2269.

[43] Unal B, Netti M C, Hassan M A, et al. Neodymium-doped tantalum pentoxide waveguide lasers[J]. IEEE Journal of Quantum Electronics, 2005, 41(12): 1565-1573.

[44] Grant-Jacob J A, Beecher S J, Parsonage T L, et al. An 11.5 W Yb∶YAG planar waveguide laser fabricated via pulsed laser deposition [J]. Optical Materials Express, 2016, 6(1): 91-96.

[45] Tan Y, Rodenas A, Chen F, et al. 70% slope efficiency from an ultrafast laser-written Nd∶$GdVO_4$ channel waveguide laser[J]. Optics Express, 2010, 18(24): 24994-24999.

[46] Nie W J, He R Y, Cheng C, et al. Optical lattice-like cladding waveguides by direct laser writing: fabrication, luminescence, and lasing [J]. Optics Letters, 2016, 41(10): 2169-2172.

[47] Liu H L, Vázquez de Aldana J R, Hong M H, et al. Femtosecond laser inscribed Y-branch waveguide in Nd∶YAG crystal: fabrication and continuous-wave lasing[J]. IEEE Journal of Selected Topics in Quantum Electronics, 2016, 22(2): 227-230.

[48] Jia Y C, Cheng C, Vázquez de Aldana J R, et al. Three-dimensional waveguide splitters inscribed in Nd∶YAG by femtosecond laser writing: realization and laser emission [J]. Journal of Lightwave Technology, 2016, 34(4): 1328-1332.

[49] Calmano T, Paschke A G, Müller S, et al. Curved Yb∶YAG waveguide lasers, fabricated by femtosecond laser inscription[J]. Optics Express, 2013, 21(21): 25501-25508.

[50] Calmano T, Müller S. Crystalline waveguide lasers in the visible and near-infrared spectral range [J]. IEEE Journal of Selected Topics in Quantum Electronics, 2015, 21(1): 401-413.

[51] Calmano T, Siebenmorgen J, Reichert F, et al. Crystalline Pr∶$SrAl_{12}O_{19}$ waveguide laser in the visible spectral region[J]. Optics Letters, 2011, 36(23): 4620-4622.

[52] Reichert F, Calmano T, Müller S, et al. Efficient visible laser operation of Pr, Mg∶$SrAl_{12}O_{19}$ channel waveguides [J]. Optics Letters, 2013, 38(15): 2698-2701.

[53] Starecki F, Bolaños W, Braud A, et al. Red and orange $Pr^{3+}$∶$LiYF_4$ planar waveguide laser [J]. Optics Letters, 2013, 38(4): 455-457.

[54] Bolaños W, Brasse G, Starecki F, et al. Green, orange, and red $Pr^{3+}$∶$YLiF_4$ epitaxial waveguide lasers [J]. Optics Letters, 2014, 39(15): 4450-4453.

[55] Lancaster D G, Gross S, Ebendorff-Heidepriem H, et al. 2.1 μm waveguide laser fabricated by femtosecond laser direct-writing in $Ho^{3+}$, $Tm^{3+}$∶ZBLAN glass [J]. Optics Letters, 2012, 37(6):

996-998.

[56] Lancaster D G, Gross S, Ebendorff-Heidepriem H, et al. Efficient 2.9 μm fluorozirconate glass waveguide chip laser[J]. Optics Letters, 2013, 38(14): 2588-2591.

[57] Lancaster D G, Stevens V J, Michaud-Belleau V, et al. Holmium-doped 2.1 μm waveguide chip laser with an output power >1 W[J]. Optics Express, 2015, 23(25): 32664-32670.

[58] McDaniel S, Thorburn F, Lancaster A, et al. Operation of Ho∶YAG ultrafast laser inscribed waveguide lasers[J]. Applied Optics, 2017, 56(12): 3251-3256.

[59] MacDonald J R, Beecher S J, Lancaster A, et al. Compact Cr∶ZnS channel waveguide laser operating at 2333 nm[J]. Optics Express, 2014, 22(6): 7052-7057.

[60] Kifle E, Loiko P, Romero C, et al. Femtosecond-laser-written Ho∶KGd($WO_4$)$_2$ waveguide laser at 2.1 μm[J]. Optics Letters, 2019, 44(7): 1738-1741.

[61] Liu H L, Jia Y C, Vázquez de Aldana J R, et al. Femtosecond laser inscribed cladding waveguides in Nd∶YAG ceramics: fabrication, fluorescence imaging and laser performance[J]. Optics Express, 2012, 20(17): 18620-18629.

[62] Liu H L, Chen F, Vázquez de Aldana J R, et al. Femtosecond-laser inscribed double-cladding waveguides in Nd∶YAG crystal: a promising prototype for integrated lasers[J]. Optics Letters, 2013, 38(17): 3294-3297.

[63] Jia Y, Dong N, Chen F, et al. Continuous wave waveguide lasers in femtosecond laser micromachined ion irradiated Nd∶YAG single crystals[J]. Optical Materials Express, 2012, 2(5): 657-662.

[64] Jia Y C, Vázquez de Aldana J R, Lu Q M, et al. Second harmonic generation of violet light in femtosecond-laser-inscribed $BiB_3O_6$ cladding waveguides[J]. Optical Materials Express, 2013, 3(9): 1279-1284.

[65] Jia Y C, Rüter C E, Akhmadaliev S, et al. Ridge waveguide lasers in Nd∶YAG crystals produced by combining swift heavy ion irradiation and precise diamond blade dicing [J]. Optical Materials Express, 2013, 3(4): 433-438.

[66] Yao Y C, Dong N N, Chen F, et al. Continuous wave waveguide lasers of swift argon ion irradiated Nd∶$YVO_4$ waveguides[J]. Optics Express, 2011, 19(24): 24252-24257.

[67] Jia Y C, Chen F, Vázquez de Aldana J R. Efficient continuous-wave laser operation at 1064 nm in Nd∶$YVO_4$ cladding waveguides produced by femtosecond laser inscription[J]. Optics Express, 2012, 20(15): 16801-16806.

[68] Liu H L, Vázquez de Aldana J R, Aguiló M, et al. Femtosecond laser-written double-cladding waveguides in Nd∶$GdVO_4$ crystal: Raman analysis, guidance, and lasing [J]. Optical Engineering, 2014, 53(9): 097105.

[69] Liu H L, Tan Y, Vázquez de Aldana J R, et al. Efficient laser emission from cladding waveguide inscribed in Nd∶$GdVO_4$ crystal by direct femtosecond laser writing [J]. Optics Letters, 2014, 39(15): 4553-4556.

[70] Ren Y Y, Dong N N, MacDonald J, et al. Continuous wave channel waveguide lasers in Nd∶$LuVO_4$ fabricated by direct femtosecond laser writing[J]. Optics Express, 2012, 20(3): 1969-1974.

[71] Liu H L, An Q, Chen F, et al. Continuous-wave lasing at 1.06 μm in femtosecond laser written Nd∶KGW waveguides[J]. Optical Materials, 2014, 37: 93-96.

[72] Liu H L, Jia Y C, Chen F, et al. Continuous wave laser operation in Nd∶GGG depressed tubular cladding waveguides produced by inscription of femtosecond laser pulses [J]. Optical Materials Express, 2013, 3(2): 278-283.

[73] Jia Y C, Dong N N, Chen F, et al. Ridge waveguide lasers in Nd∶GGG crystals produced by swift carbon ion irradiation and femtosecond laser ablation[J]. Optics Express, 2012, 20(9): 9763-9768.

[74] Ren Y Y, Vázquez de Aldana J R, Chen F, et al. Channel waveguide lasers in Nd∶LGS crystals[J]. Optics Express, 2013, 21(5): 6503-6508.

[75] Calmano T, Siebenmorgen J, Paschke A G, et al. Diode pumped high power operation of a femtosecond laser inscribed Yb∶YAG waveguide laser [Invited] [J]. Optical Materials Express, 2011, 1(3): 428-433.

[76] Siebenmorgen J, Calmano T, Petermann K, et al. Highly efficient Yb∶YAG channel waveguide laser written with a femtosecond-laser [J]. Optics Express, 2010, 18(15): 16035-16041.

[77] Jia Y C, Vázquez de Aldana J R, Chen F. Efficient waveguide lasers in femtosecond laser inscribed double-cladding waveguides of Yb∶YAG ceramics [J]. Optical Materials Express, 2013, 3(5): 645-650.

[78] Geskus D, Bernhardi E H, van Dalfsen K, et al.

Highly efficient $Yb^{3+}$-doped channel waveguide laser at 981 nm[J]. Optics Express, 2013, 21(11): 13773-13778.

[79] van Dalfsen K, Aravazhi S, Grivas C, et al. Thulium channel waveguide laser in a monoclinic double tungstate with 70% slope efficiency[J]. Optics Letters, 2012, 37(5): 887-889.

[80] van Dalfsen K, Aravazhi S, Grivas C, et al. Thulium channel waveguide laser with 1.6 W of output power and ~80% slope efficiency[J]. Optics Letters, 2014, 39(15): 4380-4383.

[81] Szela J W, Sloyan K A, Parsonage T L, et al. Laser operation of a Tm∶$Y_2O_3$ planar waveguide [J]. Optics Express, 2013, 21(10): 12460-12468.

[82] Ren Y Y, Brown G, Ródenas A, et al. Mid-infrared waveguide lasers in rare-earth-doped YAG [J]. Optics Letters, 2012, 37(16): 3339-3341.

[83] Liu X F, Guo Q B, Qiu J R. Emerging low-dimensional materials for nonlinear optics and ultrafast photonics[J]. Advanced Materials, 2017, 29(14): 1605886.

[84] Yu S L, Wu X Q, Wang Y P, et al. 2D materials for optical modulation: challenges and opportunities [J]. Advanced Materials, 2017, 29(14): 1606128.

[85] Luo Z Q, Wu D D, Xu B, et al. Two-dimensional material-based saturable absorbers: towards compact visible-wavelength all-fiber pulsed lasers [J]. Nanoscale, 2016, 8(2): 1066-1072.

[86] Zhu X, Chen S, Zhang M, et al. $TiS_2$-based saturable absorber for ultrafast fiber lasers[J]. Photonics Research, 2018, 6(10): C44-C48.

[87] Fang Y R, Ge Y Q, Wang C, et al. Mid-infrared photonics using 2D materials: status and challenges [J]. Laser & Photonics Reviews, 2020, 14(1): 1900098.

[88] Wang S X, Yu H H, Zhang H J, et al. Broadband few-layer $MoS_2$ saturable absorbers[J]. Advanced Materials, 2014, 26(21): 3538-3544.

[89] Liu Z K, Mu H R, Xiao S, et al. Pulsed lasers: pulsed lasers employing solution-processed plasmonic $Cu_{3-x}P$ colloidal nanocrystals [J]. Advanced Materials, 2016, 28(18): 3604-3542.

[90] Wang G Z, Wang K P, Szydłowska B M, et al. Ultrafast nonlinear optical properties of a graphene saturable mirror in the 2 μm wavelength region[J]. Laser & Photonics Reviews, 2017, 11(5): 1770051.

[91] Jiang X T, Liu S X, Liang W Y, et al. Broadband nonlinear photonics in few-layer MXene $Ti_3C_2T_x$ ($T$= F, O, or OH)[J]. Laser & Photonics Reviews, 2018, 12(2): 1870013.

[92] Gao P, Huang J H, Liu H G, et al. Passively $Q$-switched solid-state Tm∶YAG laser with $MoS_2$ as saturable absorber[J]. Chinese Journal of Lasers, 2018, 45(7): 0701002.
高攀, 黄见洪, 刘华刚, 等. 基于可饱和吸收体 $MoS_2$ 的固态 Tm∶YAG 被动调 Q 激光器[J]. 中国激光, 2018, 45(7): 0701002.

[93] Ma L N, Tan Y, Chen F. Pulsed waveguide laser based on thermal-control of vanadium dioxide[J]. Chinese Journal of Lasers, 2017, 44(7): 0703010.
马利男, 谭杨, 陈峰. 基于二氧化钒的热控制脉冲波导激光[J]. 中国激光, 2017, 44(7): 0703010.

[94] Novoselov K S, Mishchenko A, Carvalho A, et al. 2D materials and van der Waals heterostructures [J]. Science, 2016, 353(6298): aac9439.

[95] Bae J E, Park T G, Kifle E, et al. Carbon nanotube $Q$-switched Yb∶KLuW surface channel waveguide lasers[J]. Optics Letters, 2020, 45(1): 216-219.

[96] Ma L N, Tan Y, Wang S X, et al. Continuous-wave and $Q$-switched Yb∶YSGG waveguide laser [J]. Journal of Lightwave Technology, 2017, 35(13): 2642-2645.

[97] Cheng C, Li Z Q, Dong N N, et al. Tin diselenide as a new saturable absorber for generation of laser pulses at 1 μm[J]. Optics Express, 2017, 25(6): 6132-6140.

[98] Hakobyan S, Wittwer V J, Hasse K, et al. Highly efficient $Q$-switched Yb∶YAG channel waveguide laser with 5.6 W of average output power[J]. Optics Letters, 2016, 41(20): 4715-4718.

[99] Li Z Q, Cheng C, Dong N N, et al. $Q$-switching of waveguide lasers based on graphene/$WS_2$ van der Waals heterostructure [J]. Photonics Research, 2017, 5(5): 406-410.

[100] Ma L N, Tan Y, Akhmadaliev S, et al. Electrically tunable Nd∶YAG waveguide laser based on graphene [J]. Scientific Reports, 2016, 6: 36785.

[101] Wieschendorf C, Firth J, Silvestri L, et al. Compact integrated actively $Q$-switched waveguide laser[J]. Optics Express, 2017, 25(3): 1692-1701.

[102] Kim J W, Choi S Y, Bae J E, et al. Comparative study of Yb∶KYW planar waveguide lasers $Q$-switched by direct- and evanescent-field interaction with carbon nanotubes[J]. Optics Express, 2019, 27(2): 1488-1496.

[103] Kifle E, Loiko P, Vázquez de Aldana J R, et al. Passively $Q$-switched femtosecond-laser-written thulium waveguide laser based on evanescent field interaction with carbon nanotubes[J]. Photonics Research, 2018, 6(10): 971-980.

[104] Kifle E, Loiko P, Vázquez de Aldana J R, et al. Fs-

laser-written thulium waveguide lasers *Q*-switched by graphene and $MoS_2$ [J]. Optics Express, 2019, 27(6): 8745-8755.

[105] Loiko P, Bogusławski J, Serres J M, et al. $Sb_2Te_3$ thin film for the passive *Q*-switching of a Tm∶$GdVO_4$ laser[J]. Optical Materials Express, 2018, 8(7): 1723-1732.

[106] Tan Y, Cheng C, Akhmadaliev S, et al. Nd∶YAG waveguide laser *Q*-switched by evanescent-field interaction with graphene [J]. Optics Express, 2014, 22(8): 9101-9106.

[107] Lin H F, Tang F, Chen W D, et al. Diode-pumped tape casting planar waveguide YAG/Nd∶YAG/YAG ceramic laser [J]. Optics Express, 2015, 23(6): 8104-8112.

[108] Tan Y, Akhmadaliev S, Zhou S Q, et al. Guided continuous-wave and graphene-based *Q*-switched lasers in carbon ion irradiated Nd∶YAG ceramic channel waveguide [J]. Optics Express, 2014, 22(3): 3572-3577.

[109] Tan Y, Guo Z N, Ma L N, et al. *Q*-switched waveguide laser based on two-dimensional semiconducting materials: tungsten disulfide and black phosphorous [J]. Optics Express, 2016, 24(3): 2858-2866.

[110] Tan Y, He R Y, MacDonald J, et al. *Q*-switched Nd∶YAG channel waveguide laser through evanescent field interaction with surface coated graphene[J]. Applied Physics Letters, 2014, 105(10): 101111.

[111] Liu H L, Cheng C, Romero C, et al. Graphene-based Y-branch laser in femtosecond laser written Nd∶YAG waveguides[J]. Optics Express, 2015, 23(8): 9730-9735.

[112] Cheng C, Liu H L, Shang Z, et al. Femtosecond laser written waveguides with $MoS_2$ as satuable absorber for passively *Q*-switched lasing[J]. Optical Materials Express, 2016, 6(2): 367-373.

[113] Tan Y, Liu X B, He Z L, et al. Tuning of interlayer coupling in large-area graphene/$WSe_2$ van der Waals heterostructure via ion irradiation: optical evidences and photonic applications [J]. ACS Photonics, 2017, 4(6): 1531-1538.

[114] Cheng C, Liu H L, Tan Y, et al. Passively *Q*-switched waveguide lasers based on two-dimensional transition metal diselenide [J]. Optics Express, 2016, 24(10): 10385-10390.

[115] Tan Y, Zhang H, Zhao C J, et al. $Bi_2Se_3$ *Q*-switched Nd∶YAG ceramic waveguide laser [J]. Optics Letters, 2015, 40(4): 637-640.

[116] Tan Y, Guo Z N, Shang Z, et al. Tailoring nonlinear optical properties of $Bi_2Se_3$ through ion irradiation[J]. Scientific Reports, 2016, 6: 21799.

[117] Jia Y C, Tan Y, Cheng C, et al. Efficient lasing in continuous wave and graphene *Q*-switched regimes from Nd∶YAG ridge waveguides produced by combination of swift heavy ion irradiation and femtosecond laser ablation [J]. Optics Express, 2014, 22(11): 12900-12908.

[118] Ma L, Tan Y, Ghorbani-Asl M, et al. Tailoring the optical properties of atomically-thin $WS_2$ via ion irradiation [J]. Nanoscale, 2017, 9(31): 11027-11034.

[119] He R Y, Vázquez de Aldana J R, Chen F. Passively *Q*-switched Nd∶$YVO_4$ waveguide laser using graphene as a saturable absorber [J]. Optical Materials, 2015, 46: 414-417.

[120] Nie W J, Li R, Cheng C, et al. Room-temperature subnanosecond waveguide lasers in Nd∶$YVO_4$ *Q*-switched by phase-change $VO_2$: a comparison with 2D materials [J]. Scientific Reports, 2017, 7: 46162.

[121] Pang C, Li R, Zhang Y X, et al. Tailoring optical nonlinearities of $LiNbO_3$ crystals by plasmonic silver nanoparticles for broadband saturable absorbers[J]. Optics Express, 2018, 26(24): 31276-31289.

[122] Jia Y C, He R Y, Vázquez de Aldana J R, et al. Femtosecond laser direct writing of few-mode depressed-cladding waveguide lasers [J]. Optics Express, 2019, 27(21): 30941-30951.

[123] Choi S Y, Calmano T, Kim M H, et al. *Q*-switched operation of a femtosecond-laser-inscribed Yb∶YAG channel waveguide laser using carbon nanotubes[J]. Optics Express, 2015, 23(6): 7999-8005.

[124] Choudhary A, Beecher S J, Dhingra S, et al. 456-mW graphene *Q*-switched Yb∶yttria waveguide laser by evanescent-field interaction [J]. Optics Letters, 2015, 40(9): 1912-1915.

[125] Ren Y Y, Cheng C, Jia Y C, et al. Switchable single-dual-wavelength Yb, Na∶$CaF_2$ waveguide lasers operating in continuous-wave and pulsed regimes [J]. Optical Materials Express, 2018, 8(6): 1633-1641.

[126] Kifle E, Mateos X, Loiko P, et al. Graphene *Q*-switched Tm∶$KY(WO_4)_2$ waveguide laser[J]. Laser Physics, 2017, 27(4): 045801.

[127] Loiko P, Serres J M, Delekta S S, et al. Inkjet-printing of graphene saturable absorbers for ~2 μm bulk and waveguide lasers [J]. Optical Materials Express, 2018, 8(9): 2803-2814.

[128] Kifle E, Mateos X, Vázquez de Aldana J R, et al. Femtosecond-laser-written Tm∶$KLu(WO_4)_2$

waveguide lasers[J]. Optics Letters, 2017, 42(6): 1169-1172.

[129] Kifle E, Mateos X, Loiko P, et al. Tm∶$KY_{1-x-y}Gd_xLu_y(WO_4)_2$ planar waveguide laser passively *Q*-switched by single-walled carbon nanotubes [J]. Optics Express, 2018, 26(4): 4961-4966.

[130] Kifle E, Loiko P, Griebner U, et al. Diamond saw dicing of thulium channel waveguide lasers in monoclinic crystalline films [J]. Optics Letters, 2019, 44(7): 1596-1599.

[131] Mary R, Brown G, Beecher S J, et al. 1.5 GHz picosecond pulse generation from a monolithic waveguide laser with a graphene-film saturable output coupler[J]. Optics Express, 2013, 21(7): 7943-7950.

[132] Ren Y Y, Brown G, Mary R, et al. 7.8-GHz graphene-based 2-μm monolithic waveguide laser [J]. IEEE Journal of Selected Topics in Quantum Electronics, 2015, 21(1): 395-400.

[133] Thorburn F, Lancaster A, McDaniel S, et al. 5.9 GHz graphene based *Q*-switched modelocked mid-infrared monolithic waveguide laser[J]. Optics Express, 2017, 25(21): 26166-26174.

[134] Li Z Q, Zhang Y X, Cheng C, et al. 6.5 GHz *Q*-switched mode-locked waveguide lasers based on two-dimensional materials as saturable absorbers [J]. Optics Express, 2018, 26(9): 11321-11330.

[135] Li Z Q, Dong N N, Cheng C, et al. Enhanced nonlinear optical response of graphene by silver-based nanoparticle modification for pulsed lasing[J]. Optical Materials Express, 2018, 8(5): 1368-1377.

[136] Pang C, Li R, Li Z Q, et al. Mode-locked lasers: lithium niobate crystal with embedded Au nanoparticles: a new saturable absorber for efficient mode-locking of ultrafast laser pulses at 1 μm[J]. Advanced Optical Materials, 2018, 6(16): 1870065.

[137] Li R, Pang C, Li Z Q, et al. Fused silica with embedded 2D-like Ag nanoparticle monolayer: tunable saturable absorbers by interparticle spacing manipulation [J]. Laser & Photonics Reviews, 2020, 14(2): 1900302.

[138] Okhrimchuk A G, Obraztsov P A. 11-GHz waveguide Nd∶YAG laser CW mode-locked with single-layer graphene[J]. Scientific Reports, 2015, 5: 11172.

[139] Li Z Q, Dong N N, Zhang Y X, et al. Mode-locked waveguide lasers modulated by rhenium diselenide as a new saturable absorber[J]. APL Photonics, 2018, 3(8): 080802.

[140] Choi S Y, Calmano T, Rotermund F, et al. 2-GHz carbon nanotube mode-locked Yb∶YAG channel waveguide laser[J]. Optics Express, 2018, 26(5): 5140-5145.

[141] Khurmi C, Hébert N B, Zhang W Q, et al. Ultrafast pulse generation in a mode-locked erbium chip waveguide laser[J]. Optics Express, 2016, 24(24): 27177-27183.

[142] Grivas C, Ismaeel R, Corbari C, et al. Generation of multi-gigahertz trains of phase-coherent femtosecond laser pulses in Ti∶sapphire waveguides [J]. Laser & Photonics Reviews, 2018, 12(11): 1800167.

[143] Wang S X, Pang C, Li Z Q, et al. 8.6 GHz *Q*-switched mode-locked waveguide lasing based on $LiNbO_3$ crystal embedded Cu nanoparticles [J]. Optical Materials Express, 2019, 9(9): 3808-3817.

[144] Pang C, Li R, Li Z Q, et al. Copper nanoparticles embedded in lithium tantalate crystals for multi-GHz lasers [J]. ACS Applied Nano Materials, 2019, 2(9): 5871-5877.

[145] Li Z Q, Li R, Pang C, et al. 8.8 GHz *Q*-switched mode-locked waveguide lasers modulated by $PtSe_2$ saturable absorber[J]. Optics Express, 2019, 27(6): 8727-8737.

[146] Ponarina M V, Okhrimchuk A G, Rybin M G, et al. Dual-wavelength generation of picosecond pulses with 9.8 GHz repetition rate in Nd∶YAG waveguide laser with graphene [J]. Quantum Electronics, 2019, 49(4): 365-370.

[147] Li Z Q, Li R, Pang C, et al. $WSe_2$ as a saturable absorber for multi-gigahertz *Q*-switched mode-locked waveguide lasers [Invited] [J]. Chinese Optics Letters, 2019, 17(2): 020013.

[148] Choudhary A, Lagatsky A A, Kannan P, et al. Diode-pumped femtosecond solid-state waveguide laser with a 4.9 GHz pulse repetition rate [J]. Optics Letters, 2012, 37(21): 4416-4418.

[149] Lagatsky A A, Choudhary A, Kannan P, et al. Fundamentally mode-locked, femtosecond waveguide oscillators with multi-gigahertz repetition frequencies up to 15 GHz [J]. Optics Express, 2013, 21(17): 19608-19614.

[150] Choudhary A, Dhingra S, D′Urso B, et al. Graphene *Q*-switched mode-locked and *Q*-switched ion-exchanged waveguide lasers[J]. IEEE Photonics Technology Letters, 2015, 27(6): 646-649.

[151] Jiang X T, Gross S, Zhang H, et al. Bismuth telluride topological insulator nanosheet saturable absorbers for *Q*-switched mode-locked Tm∶ZBLAN waveguide lasers [J]. Annalen Der Physik, 2016, 528(7/8): 543-550.